



Predictive modelling of land use land cover dynamics for a tropical coastal urban city in Kerala, India

Ande Bhuvaneswari Devi¹ · Dhritilekha Deka¹ · Thayyil Davood Aneesh² · Reji Srinivas² · Archana M. Nair¹

Received: 11 August 2021 / Accepted: 17 February 2022 / Published online: 22 February 2022
© Saudi Society for Geosciences 2022

Abstract

Land use land cover (LULC) changes act as global environmental drivers, and therefore, LULC change analysis has become the primary concern for the monitoring agencies. This study aims to project the land use and land cover (LULC) by analysing the change rate in the past, forecasting the near, middle, and far future scenarios of Cochin, a highly urbanised coastal city of Kerala, India. The natural land resources, specifically the wetlands, are undergoing adverse changes to meet the growing demands of industrialisation and basic anthropological necessities in Kochi, causing negative feedback on the environment. We performed the maximum likelihood classification technique on a series of Landsat imageries at five different times. We forecasted LULC scenarios of 2045, 2073, and 2100 using Modules for Land Change Evaluation (MOLUSCE) in QGIS. The model simulated LULC was validated by comparing the observed LULC 2020 with the simulated one. The model demonstrates acceptable LULC dynamics with an overall accuracy of 87.5%. The simulated future LULC scenarios illustrate a sweeping increase in the built-up lands and shrinkage of natural land covers such as agricultural lands, forests, fallow lands, and water bodies. The urban growth indicator based on impervious to pervious ratio (IPR) confirms the extreme transformations of the area in terms of urbanisation. The destructive effect of urbanisation on natural land cover is likely to be predominantly more alarming in the near future than in the far. The leads of this study urge the necessity to establish appropriate urban planning and management policies for sustainable environmental conservation.

Keywords Land use land cover · GIS · Multi-layer perceptron neural network · Cellular automata (CA) · Markov chain

Introduction

Intense anthropogenic activities such as urbanisation and industrialisation significantly influence the demographic features and alterations of the physical landscape. These activities adversely affect the Earth's natural environment, especially the hydrosphere and lithosphere (Fichera et al. 2017; Patra et al. 2018; Singh et al. 2015). In the current scenario, rapid socio-economic growth has resulted in a significant shift in global land use and land cover (LULC) (Q. Wang

et al. 2021a, b, c). In modern human history, land expansion in urban locations is one of the highest noticeable, unalterable, and rapid forms of LULC change. Therefore, urban land expansion is the root cause of many environmental and societal modifications (Gao and O'Neill 2020). Moreover, rapid urbanisation due to population and economic development threatens natural resources (Mohan et al. 2011). Changes in LULC results in significant global and regional changes in climate variables (Al et al. 2020; Li et al. 2020; Patra et al. 2018), groundwater level (Nath et al. 2021; Patra et al. 2018), hydrology (Chanapathi and Thatikonda 2020; Yuan 2008; Zhang and Schilling 2006), water quality (Tahiru et al. 2020; Yuan 2008), estuarine (Dipson et al. 2015), and air quality (K. Wang et al. 2021a, b, c). Though land use is conventionally considered a local concern to the environment, it is gradually transforming as a global dynamism (Samal and Gedam 2013). Therefore, a thorough analysis of the dynamics of the land-cover alterations generated by urbanisation is essential in enabling sustainable regional land use

Responsible Editor: Biswajeet Pradhan

✉ Nair Archana M.
nair.archana@iitg.ac.in

¹ Department of Civil Engineering, Indian Institute of Technology, Guwahati 781039, Assam, India

² National Centre for Earth Science Studies, Thiruvananthapuram 695031, Kerala, India

management and adaptation to the resultant environmental modifications (Patra et al. 2018; Wang et al. 2021a, b, c).

In the last five decades, the population has doubled, with India ranked second in World's population. However, the megacities of India are not planned to meet this scale of population increase (Nath et al. 2021). Consequently, development activities such as urbanisation, population growth, and industrialisation are forcing alterations on LULC patterns across the country. Kerala state on the west coast of India is famous for tourism, physiography, and biodiversity. It accommodates a series of lagoons and estuaries, with a high population density of 860 persons per km² (Sreelekshmi et al. 2021). During the 2001–2011 period, the state has witnessed an urban population growth of 92.72%. With the increase in the standards of living, there has been an upsurge in the employment demand along with better opportunities for education and health facilities, leading to the migration from rural areas towards urban areas across the state, resulting in an increased area under urbanisation (State Urbanisation Report 2012; Praveen and Nair 2017). A distinct shift in land use is reported in the state, with a decline in area under agroforest and rise in area under non-agricultural use with the expansion in migration accompanied by increased remittances used for land, infrastructures, and roads (Fox et al. 2017; Johnson 2018). Many districts in the state, such as Alappuzha (Vadrevu et al. 2015), Wayanad (John et al. 2020), and Kollam (Sajeew and Subramanian 2003), have emphasised alterations in the land use patterns over time due to human encroachments. Ernakulam district, a part of erstwhile Kochi, represents the modern phase of Kerala. Kochi has a prominent place in the history of Kerala's age-old trade links with the rest of the world and is referred to as the queen of the Arabian Sea. In the present study, we analysed the changes in the LULC pattern for the past three decades of Cochin urban agglomeration within Ernakulam district.

Satellite-based remote sensing (RS) data with GIS techniques are found to be most effective in characterising the LULC changes in the spatiotemporal framework and integrating the associated driving factors (Aneesha Satya et al. 2020; Fichera et al. 2017; Singh et al. 2015). The recent researchers are focused on the model-based LULC trends and the projection of future LULC scenarios, especially in analysing various natural events (Amini Parsa and Salehi 2016). Several models exist to forecast and simulate land use transition dynamics based on conceptual (Gao and O'Neill 2020) and computational methods (Fondevilla et al. 2016). Multi-layer perceptron (MLP) neural network (Mozumder et al. 2016; Yonaba et al. 2021), logistic regression (LR) (Mozumder et al. 2016), weighted instance-based learning (Mozumder et al. 2016), and coupled models such as Markov cellular-automata (Amini Parsa and Salehi 2016; Chanapathi and Thatikonda 2020; Rodrigues and Guimar 2021; Sang et al. 2011; Singh et al. 2015; Waseem et al.

2015), LR-CA-Markov (Q. Wang et al. 2021a, b, c), artificial neural network-CA (Rahman et al. 2017), and MLP-CA-Markov (Al et al. 2020; Aneesha Satya et al. 2020; Guidigan et al. 2019; Ibrahim and Ludin 2015) are prevalent models to forecast LULC. The existing LULC models and forecasts differ in the conceptual context, scenario frameworks, thematic emphases, spatial features, and modelling approaches (Sohl et al. 2016).

The study area is growing exponentially with the emergence of the service sector and industries, reflecting the urban growth patterns displayed by most Indian cities. Any major or minor changes in LULC induce severe damage at a massive scale in the coastal ecosystems of the study area due to the prevailing sensitive ecology (Dipson et al. 2015; Rafeeqe et al. 2020). Apex court of India has recently ordered the demolition of four big apartment complexes, violating coastal zone regulations. Hence, analysing the evolving pattern of LULC in the past, and modelling the future, offers a unique opportunity to analyse and improve the current and forthcoming land use policies (Rahman et al. 2017). Therefore, a study on LULC dynamics of present and future will reduce the risk of vulnerability and address the issues related to conservation of natural ecosystem and urban planning of the district, through the proper intervention of sustainable land resource management policies. In this study, We analysed the spatiotemporal variations of LULC from 1994 to 2020. We predicted the scenarios for the near (2045), middle (2073), and far future (2100) for the benefit of sustainable futuristic urban development and management. This study applied maximum likelihood classification (MLC) on Landsat data for LULC mapping and change detection. We used MOLUSCE (Modules for Land Use Change Evaluation) model that works in the QGIS interface for future LULC forecasts. The forecasted LULC scenarios of near, mid, and far future times can support an effective land management policy.

Material and methodology

Study area

The study area is Kochi, the coastal urban city of Ernakulam district in Kerala state of India that lies between 9° 48' N and 10° 16' N latitude and 76° 10' E and 76° 29' E longitude covering an area of 910 km² (Fig. 1). The climate regime is tropical, with mean monthly temperature varying between 23 and 32 °C, and annual precipitation ranging between 3200 and 3500 mm. Vembanad Lake system, listed in Ramsar wetlands, is partly in Ernakulam district. The portion of this Lake in and around the Kochi mainland is known as Kochi Kayal. Islands named Vypin, Mulavukad, Vallarpadam, and Willingdon contained by the Vembanad

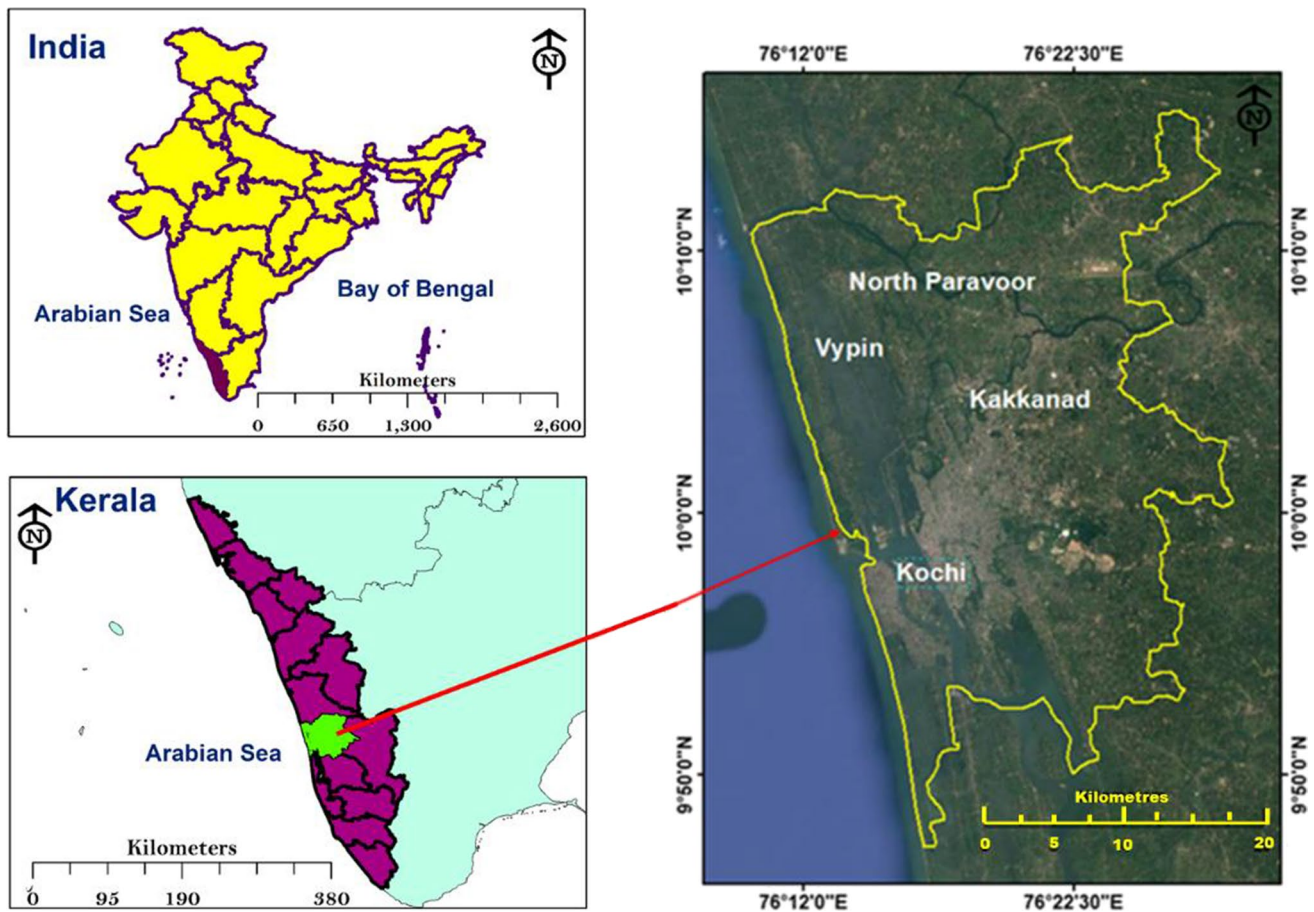


Fig. 1 Location map of the study area (base map source: Google Earth © imagery of Cochin, Ernakulum)

lake system are (Department of Mining and Geology 2016) within the study area. The Vembanad lake system makes this area prominent on the world tourism map. The study area is the economic capital of Kerala and therefore showed steady growth in urbanisation since independence. The rapid industrial growth in this area during the recent past could be attributed to improved transportation services, including a major international airport, international container transshipment terminal, and harbour terminal within the vicinity (George 2016).

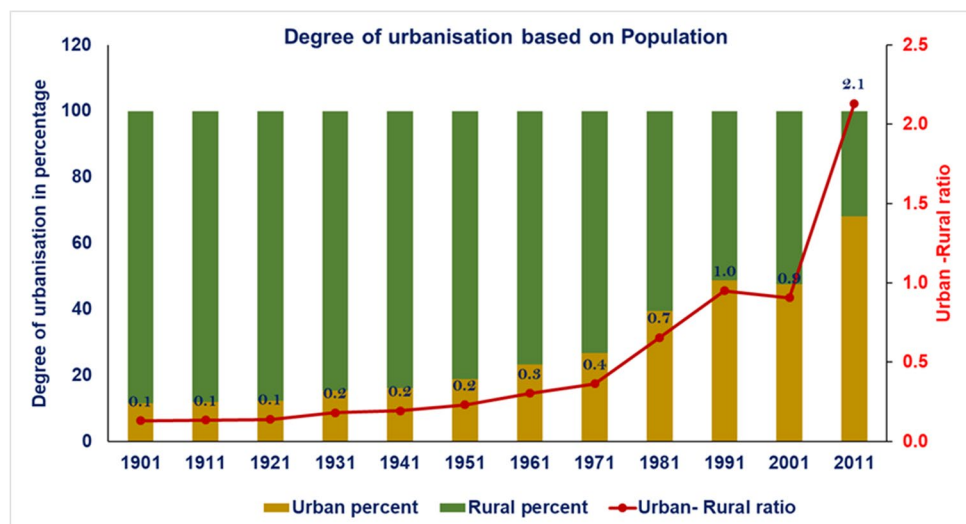
About 68% of the population of Ernakulam district live in the Kochi urban agglomeration, and hence is the highest populated city in Kerala (Thomas 2017). Ernakulam registered about a 43% increase in urban population from 2001 to 2011. Figure 2 depicts the process of urbanisation in the Ernakulam district. According to Datta (2006), the ratio of people who live in urban areas is referred to as the degree of urbanisation. In the current study area, the degree of urbanisation was measured using urban and rural population percentage and urban–rural population ratio (Fig. 2). An alarming situation is evident in the economic base of the state. According to the Department of Town and Country

Planning report in 2011, the study area shows a very prominent declining trend in the primary sector, which comprises the agricultural labourers and cultivators, in contrast to the service sector/tertiary sector. It is apparent that during 2001–2011, the graph of urban growth shows a drastic increase in the total population at a steady rate (Fig. 2).

Data collection and preparation

We generated LULC maps using multi-temporal Landsat collection-2 level-2 (Landsat 5TM and Landsat 8) satellite imagery. Our analysis utilised Landsat satellite images of 30 m spatial resolution for the following years: 1994, 2002, 2008, 2015, and 2020, obtained from the United States Geological Survey (USGS) website. All the images were geometrically and radio-metrically corrected and projected with WGS 1984 UTM Zone 43 N coordinate system. We used the MLC technique for feature extraction from Landsat images. The secondary ancillary datasets, such as socio-economic data (population density), topographic factor (slope and DEM), and human–geographic data (distance from roads and water bodies), were utilised as land

Fig. 2 Urbanisation trend in Ernakulam District from 1901 to 2011 (Source: Kerala Census 2011)



use dynamics or drivers (Chanapathi and Thatikonda 2020; Yonaba et al. 2021). The maps generated from secondary ancillary datasets for the study area are depicted in Fig. 3. The SRTM DEM for the study area was acquired from the USGS (website: <http://srtm.usgs.gov/>). The Survey of India topographical sheets were digitised to delineate the drainage and major road networks, whereas the population statistics were acquired from the Kerala State Census website for 2011. The Euclidean distance tool in ArcGIS was used to obtain the distance from the main road and water body variable (Rahman et al. 2017).

Generation of LULC maps with supervised classification technique

The classified LULC maps for the years 1994, 2002, 2008, 2015, and 2020 were generated from the satellite data with the MLC technique in the Arc GIS platform. This classification method is popular and robust due to the minimal chances of misclassification (Sun et al. 2013; Sisodia et al. 2014). From the analysis of the spectral properties of the Landsat imageries and field observation, we identified five major LULC categories in the present study area, viz., forest (forest, rubber/coconut), agricultural lands (agricultural fields/shrubs, grass, parks), water bodies, built-up lands (high intensity and low intensity), and fallow lands. The ground truth is based on field investigations conducted from 2014 to 2016 validated using Google Earth-based observations. We have trained the MLC approach with appropriate signature training sets for each feature from the satellite image, and the LULC maps were generated for the corresponding years. Subsequently, each pixel is assigned to the class with the highest likelihood of association based on variance and covariance spectral response patterns (Q.Wang et al. 2021a, b, c). The error matrix, overall accuracy, Kappa

coefficient technique was adopted to assess the accuracy of classified LULC maps of Cochin using 170 randomly selected sampling points. The binomial probability theory was applied to decide the size of the sampling points (Congalton 1991; Yonaba et al. 2021). The points were selected in such a way that they cover each LULC class in almost equal proportion and from all parts of the study area. Furthermore, the error matrix was constructed to evaluate the accuracy of the classified LULC maps (Foody 2002).

Markov chain analysis in estimation of transition probabilities

Our study utilised the stochastic Markov chain process that works on the philosophy that the future event occurrences mainly depend on the present state of the event and are independent of the past state (Unwin et al. 1977). The Markov chain process can quantify the conversion of the land use categories and the transition rates (Sang et al. 2011). The prediction of future LULC using Markov chain is achieved by analysing two different temporal LULC maps. These maps can provide insights into the transition from one state (j) of a system at time (t_{n+1}) to another state that is predicted from the state (i) of system at time (t_n) (Unwin et al. 1977). The probability of alterations from a particular state to a different state is transition probability (P_{ij}). Temporal LULC maps can provide insights into the transition from one state (j) of a system at the time (t_{n+1}) to another state, which is predicted from the state (i) of the system at the time (t_n) (Unwin et al. 1977).

$$P_{ij} = \frac{n_{ij}}{n_i} \quad (1)$$

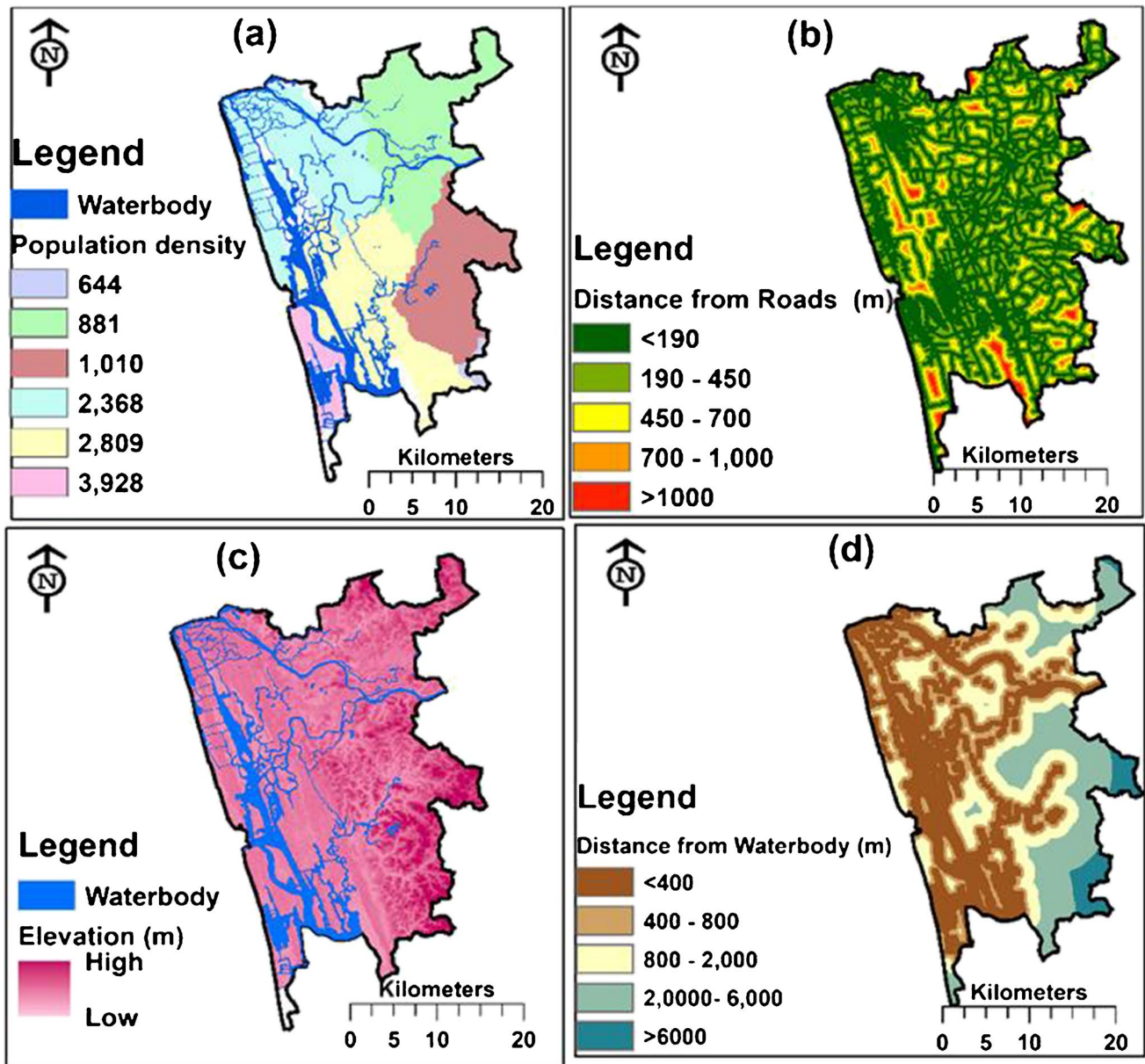


Fig. 3 Driving factors of LULC changes. **a** Population density (persons/km²) map. **b** Distance from roads. **c** Elevation map. **d** Distance from water bodies

where n_{ij} is the total number of pixels of class i transformed during the transition period, and n_j is the number of pixels changed from class i to class j .

The transition probability matrix (P_{ij}) describes the probability of changing LULC from one type to another, represented as matrix P .

$$P = P_{ij} = \begin{bmatrix} P_{11} & P_{12} & P_{13} \\ P_{21} & P_{22} & P_{23} \\ P_{31} & P_{32} & P_{33} \end{bmatrix} \tag{2}$$

where P_{ij} represents the state of the probability of a transition from i to j .

A Markov chain forecast step is illustrated here using conditional probability theory and the Markov process (Aneesha Satya et al. 2020).

$$S(t_{n+1}) = P_{ij} * S(t_n) \tag{3}$$

where $S(t_{n+1})$ represents the land use status at the time t_{n+1} and $S(t_n)$ land use status at the time t_n .

In this study, LULC was modelled with a QGIS plugin known as MOLUSCE. It is intended for analysing and

simulating existing and future LULC (Guidigan et al. 2019). The MOLUSCE plugin is an integration of well-known modelling algorithms and simulation approaches. The modelling algorithms can model the LULC change transition potential. The probability of one land cover category shifting to another is transition probability (Reddy et al. 2017). In the MOLUSCE module, four different modelling algorithms exist to calculate transition potential, viz., multilayer perceptron (MLP) neural network, multi-criteria evaluation (MCE), weights of evidence (WoE), and logistic regression (LR). The simulation of the LULC map is generated based on the cellular-automata (CA) Markov chain approach. MOLUSCE has mathematical and arithmetical progression, which will be helpful in accurate landscape analysis (Aneesha Satya et al. 2020). In all algorithms, LULC data was used as an input in deriving LULC transitions. MLP is a suitable global parametric model for simulating LULC changes to analyse the spatial drivers, which indicate the non-linear land transformation (Mozumder et al. 2016; Yang et al. 2016). The CA model is quite popular and gives the spatiotemporal framework for the LULC simulation of a complex system (Sang et al. 2011; Yang et al. 2016).

The essential inputs fed into the model for the current study include LULC maps (1994, 2008, 2015, and 2020), population density, slope and DEM, and distance from roads and water bodies. The time sequence from the Markov and the spatial estimation with the CA theory is effective in accurate spatiotemporal pattern simulation in the CA–Markov model (Sang et al. 2011). Hence, we utilised the combination of the MLP-CA-Markov models to analyse the spatial interaction triggered by current LULC and the forecasting of future LULC, which will be helpful in viable land resource planning and management.

Driving factors of LULC changes

The selection of the drivers of LULC changes plays a key role in the modelling of LULC changes. In the current study, socio-economic data (population density), topographic factor (slope and DEM), and human–geographic or proximity data (distance from roads and water bodies) were utilised as land use dynamics or drivers. The rise and decline of the human population have a massive effect on the LULC patterns of a region (Kafy et al. 2021). In particular, random urban population expansion and migration from other parts of India were observed for the last three decades in the study area. Therefore, population density is considered as one of the major driving factors of LULC changes. Topography will play a crucial role in development activities such as urbanisation, industrialisation, and agricultural intensification (Rahman et al. 2017; Sankarrao et al. 2021). Generally, the plain areas have more probability for urban expansion than sloped regions. The parameters like elevation and slope

(derived from the DEM) are also considered as drivers in the model. Other drivers, such as distance from roads and water bodies, are significant in land use change because they provide access to resources (Aneesha Satya et al. 2020; Guidigan et al. 2019; Leta et al. 2021; Sankarrao et al. 2021). All the vector files of driving factors were rasterised in ArcGIS. The driver factor maps were normalised and given a continuous suitability scale ranging from 0 to 255, with 0 being the least suitable region for LULC change and 255 representing the most appropriate.

Before examining the LULC transitions between the various periods, the influence of different driving variables on the LULC changes was analysed using Cramer's statistics (V). The strength of the correlation between different driver variables which causes the changes in LULC is analysed using Cramer's statistics by considering the Chi-square values (Hakim et al. 2019; Sankarrao et al. 2021). Cramer's statistics range from 0 (no relation between the variables) to 1 (perfect relation between the variables) (Reddy et al. 2017). Only driving factors with values greater than 0.15 (Cramer's statistics) were considered for modelling in this study (Reddy et al. 2017). A detailed description of the mathematical incorporation of driving factors in LULC modelling is given in standard literature (Gharaibeh et al. 2020; Reddy et al. 2017; Sankarrao et al. 2021).

Modelling transition potential of each class using MLP

An interrelated group of artificial neurons in ANN can process the information for computation with a connectionist approach. Highly parallel information processing is carried out for the hierarchical structure of neural networks, which are organised as interconnected units. Each layer consists of nodes/neurons which are inter-connected with neurons of adjacent layer weightage. The interactions among the linked neurons and the alterations of the weights associated with the linkages are the critical aspects of ANN (Aneesha Satya et al. 2020). Any modifications in the weightage depend on the input data and the anticipated outcome from the network. This whole procedure is known as the learning process of a network resulting in the transition probability matrix that depicts the direction in which land use types are transferred (Jogun et al. 2019).

The MLP is the most common neural network that contains three-layer types: input, hidden, and output (Pijanowski et al. 2002). These neural networks are trained with a standard backpropagation algorithm, and the local transition rules are applied for discovering the local transition rules of CA (Yang et al. 2016). It can model the multiple transitions of LULC for a period with a considerable number of driving factors (Aneesha Satya et al. 2020; Jogun et al. 2019; Yonaba et al. 2021). The identified main driving factors for

land use changes for this study are population density, distance from roads, water bodies, DEM, and slope (Fig. 3). The MLP algorithm was fed with input raster images of 2008 and 2015, along with the five driving factors for the calibration. The algorithm training was carried out for 100 iterations with a neighbourhood value of 3×3 (9 pixels), a learning rate of 0.001 with ten hidden layers in addition to 0.050 momentum value. The output of ANN represented the likelihood of change from one LULC type into another type. A zero value of change probability indicates “no chances” to change, whereas a unit value indicates the “highest chances” of modification (Pijanowski et al. 2002).

Modelling of future LULC with CA

The CA simulation used in the study is based on the Markov chain analysis and its change in the neighbourhood (Jogun et al. 2019). The CA–Markov model is one of the most extensively adopted approaches for modelling spatiotemporal dynamics of LULC patterns to assist sustainable land use development (Reddy et al. 2017; Rodrigues and Guimar 2021; Sang et al. 2011; Sankarrao et al. 2021). It is an integration of CA and transition probability matrix generated by the cross-tabulation of two different images. The model (MLP algorithm) calculates the transition probabilities of each transition category, whereas the simulator (CA) constructs the raster of the most probable transition. The initial state raster (current LULC), driving factor raster, and transition potentials are inputs to CA in MOLUSCE.

Cellular automation is a cellular entity based on the concept of proximity. The state of each cell was determined by the spatial and temporal state of its neighbouring cells (Reddy et al. 2017). The following equation is used to express the CA model (Wang et al. 2021a, b, c).

$$S_{ij}^{t+1} = f(S_{ij}^t, N_{ij}^t, V) - \quad (4)$$

where t and $t+1$ are the starting and ending times of the simulation, respectively. S_{ij}^{t+1} and S_{ij}^t are the state of the cell in row i and column j at $t+1$ and t . N_{ij}^t is the state of neighbours of the cell in row i and column j at time t . V is the set of suitability factors; f is the transition rule.

The LULC map of 2015 was used as the base map for the simulation of LULC 2020 using the CA–Markov approach. Driving factors and transition probabilities from 2008 to 2015 were used to simulate LULC 2020. Furthermore, we validated the model prediction using the observed LULC map of 2020 with respect to various kappa statistical components. Some of the kappa statistics are kappa for location (K_{loc}), which enhances the model’s ability to predict the change of locations, whereas the overall kappa was used to assess the model’s overall performance ($K_{Overall}$) (Yonaba et al. 2021). Consequently, the LULC of future scenarios for

2045, 2073, and 2100 were simulated with the calibrated and validated MLP–CA–Markov model using the base map of 2020 and transition probabilities from 1994 to 2020.

Future LULC dynamic degree estimation

We have analysed the spatiotemporal dynamics of future LULC (FLULC) patterns for various periods ranging from 2020 to 2100. The rate of gain/loss in each LULC type with image differencing (ID) method for the future with three cases of 2045–2073, 2073–2100, and 2020–2100 has been estimated. We adopted a dynamic degree (DD) model approach in representing FLULC change in terms of the spatiotemporal characteristics. The DD of LULC was estimated with the following Eq. (5) (Nath et al. 2020).

$$D = \frac{A_b - A_a}{T} \times 100\% \quad (5)$$

which denotes the rate of change; A_a is the area in the initial year; A_b is the area in the terminal year; and T is the temporal scale. In our case, the time comparisons are 26, 28, 27, and 80 years, respectively.

Results and discussion

The spatiotemporal variation in LULC of the study area showed an increase in built-up land from 9.31% in 1994 to 33.23% in 2020. The map representation of the feature distribution from multi-temporal image data for years 1994, 2002, 2008, 2015, and 2020 is displayed in Fig. 4. Based on the percentage reduction in area, the natural forest cover reduced from 34.06 to 27.72%, agricultural lands reduced from 30.23 to 17%, fallow lands reduced from 10 to 6.9%, and water bodies reduced from 16.3 to 15.13% during 1994–2020, as illustrated in Fig. 5 with details in Table 1. The percentage area coverage of built-up showed a steep increase from 1994 to 2020, while all other feature classes showed a decrease in the percentage area coverage, with forest cover showing the highest degree of depletion. The validity of the classification was analysed using Kappa statistics (Lu et al. 2019) and is detailed in Table S1. Classification accuracy calculated based on the classified images obtained using multi-temporal Landsat images from 1994 to 2020 is more than 80%, as described in Table S1.

In this work, the temporal Landsat images (1994, 2002, and 2015) were analysed at a decadal time interval starting from 1994 to analyse the historical changes in LULC. To maintain the quality of satellite image time series, efforts were made to consider images from a particular month for different period. In this study, relatively cloud-free April month was considered to maintain similarity in inter cluster

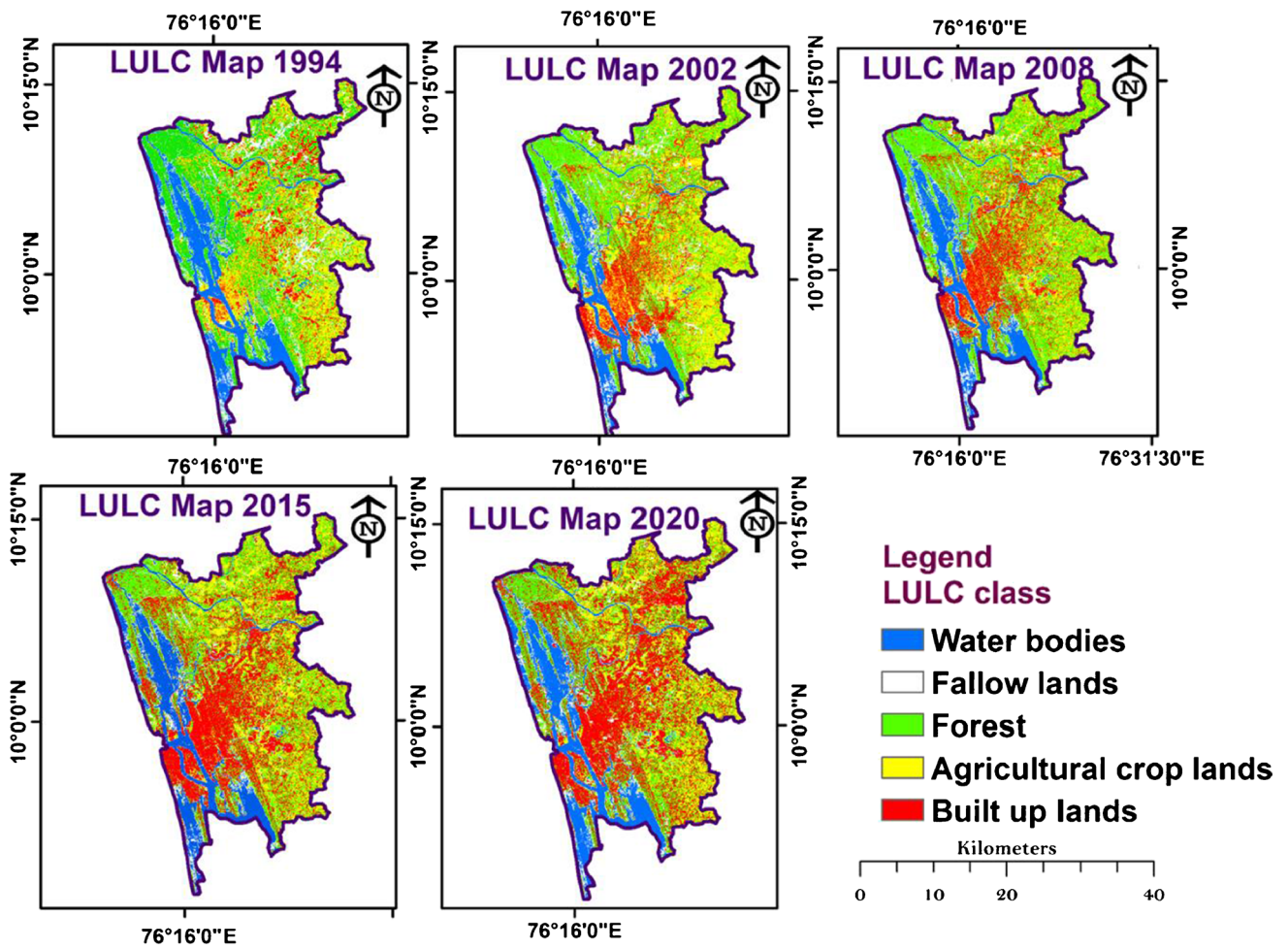
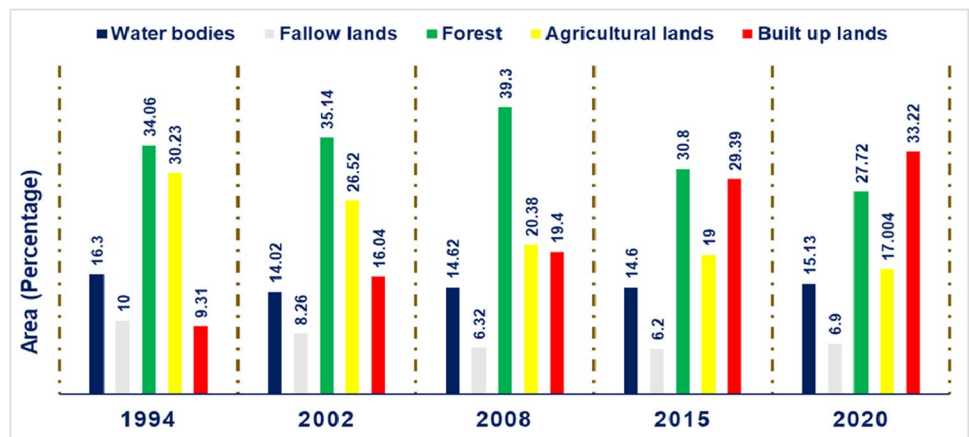


Fig. 4 Map illustration of LULC feature distribution in the study area. a Year 1994. b Year 2002. c Year 2008. d Year 2015. e Year 2020

Fig. 5 Spatiotemporal dynamics in each LULC feature between 1994 and 2020



and intra cluster variability. For example, to understand the decadal transformation in agricultural land or natural land cover such as forest cover or water bodies, it is always better to use the image from a particular season as seasonal changes are reflected in the image for such land cover

classes. If we deliberate decadal period strictly, we have to consider images of year 2004 and 2014 instead of 2002 and 2015. However, in this study, to maintain the image clarity and quality of the Landsat images used for image classification, Landsat image from 2002 was used instead of 2004

Table 1 Areal statistics of LULC features in the various period between 1994 and 2020

Class name	LULC- 1994			LULC-2002			LULC- 2008			LULC-2015			LULC- 2020		
	Area (sq. km)	Percentage (%)	Area (sq. km)	Percentage (%)	Area (sq. km)	Percentage (%)	Area (sq. km)	Percentage (%)	Area (sq. km)	Percentage (%)	Area (sq. km)	Percentage (%)	Area (sq. km)	Percentage (%)	
WB	147.57	16.3	125.38	14.02	131.82	14.62	131.83	14.6	136.37	15.13					
FL	90.17	10	74.51	8.26	57.93	6.32	55.93	6.2	62.27	6.9					
F	306.98	34.06	316.7	35.14	354.93	39.3	277.72	30.8	249.8	27.72					
AG	272.44	30.23	239.08	26.52	183.51	20.38	170.85	19	153.22	17.004					
BUL	83.94	9.31	144.57	16.04	174	19.4	264.95	29.39	299.43	33.22					

and 2015 was used instead of 2014. This is due to the unavailability of cloud-free and noise-free Landsat image data for the study area corresponding to 2004 and 2014. For the model calibration, we have considered five-year interval of Landsat data (2010, 2015, and 2020). Similar to the reasons cited above, we considered Landsat image of 2008 instead of 2010. Therefore, LULC map of 2008 and 2015 were analysed to create change scenarios for 2020, whereas 2020 data was used for the model validation.

Change detection analysis was performed to analyse the rate of change in each LULC class from 1994 to 2020. The annual change rate in each LULC class is known as dynamic degree (DD) and was computed with Eq. (5). The annual change rates for the five LULC classes are found to be 0.71%, 1.68%, 1.19%, 0.26%, and 9.87%, respectively (Table 2). However, the yearly proportion of transformation computed using Eq. (5) is inconsistent between 1994 and 2002, 2002 and 2015, and 2015 and 2020, as shown in Fig. 6. We observed an annual decline rate of 1.74% in water bodies during 1994–2002, an increasing rate of 0.31% in 2002–2015, and 0.72% in 2015–2020. The fallow lands show a decreasing rate of 2.17% in 1994–2002, and 1.92% in 2002–2015. However, for 2015–2020, fallow lands showed an increase of 2.25%. Our analysis showed that forest cover indicated a positive trend of 0.39% during 1994–2002 and a declining trend of 0.95% in 2002–2015 with a maximum annual degradation rate of 2% in 2015–2020. We observed a continuous degradation in different periods at different rates in agricultural lands, such as 1.68% in 1994–2002, 1.53% in 2002–2015, and 2.18% in 2015–2020. The maximum increasing rate of 9.03% for built-up land was witnessed during the 1994–2002 period, and the next maximum annual increasing rate of 6.4% was reported in 2002–2015, followed by 2.6% in 2015–2020. Rapid urbanisation is the major cause for reducing agricultural lands, fallow lands, forest, and water bodies evident from the net gain in the rate of change for built-up lands. Shaji et al. (2017) reported a similar observation.

The gain or loss in the areal coverage for each feature class, as shown in Fig. 6, indicates the expected pattern of an increasing trend in built-up lands and reduction in natural cover for all the phases. However, we found an atypical behaviour for certain classes during particular time intervals. We observed that forest cover increased by 0.4% in 1994–2002, and water bodies increased by 0.32% between 2002 and 2015, which could be attributed to the difference in the images used in the derivation of the particular LULC maps. An analysis on the trend observed for the changes in water bodies indicated a positive trend of 0.73% during 2015–2020. A possible explanation might be the landcover alterations post-2018 flood in the region, which is considered as the largest flood of the century. The increase in fallow lands (2.26%) for the same interval was reported, and

Table 2 LULC dynamics and annual change rate (%) estimation in LULC for various phases from 1994 to 2020

Year/LULC	1994–2008		2008–2015		2015–2020		DD (%) between different time periods			
	Area (km ²)	(Δ %)	Area (km ²)	(Δ %)	Area (km ²)	(Δ %)	1994–2002	2002–2015	2015–2020	1994–2020
Water bodies	-15.72	-1.74	0.01	0.0007	4.56	0.5	-1.75	0.32	0.73	-0.28
Fallow lands	-33.1	-3.67	-1.1	-0.12	6.21	0.7	-2.18	-1.92	2.26	-1.19
Forest	47.95	5.32	-77.2	-8.56	-28.38	-3.14	0.40	-0.95	-2.00	-0.72
Agricultural lands	-89.26	-9.9	-12.66	-1.4	-18.03	-2	-1.53	-2.18	-2.10	-1.68
Built-up lands	90.13	10	90.96	10.09	35.64	3.94	9.04	6.40	2.61	9.88

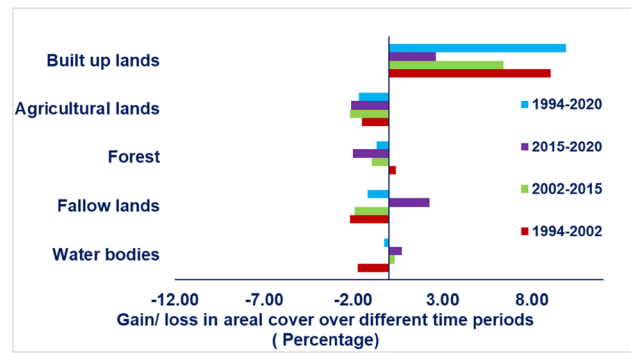


Fig. 6 Annual change rates in the areal cover of LULC categories for different periods

this could indicate the expansion of fallow lands at the cost of forest or agricultural lands for the establishment and expansion of urban features.

Transitional potentials in the LULC dynamics

Multilayer perceptron (MLP) neural network-based transitional potential model calculates transition probabilities among different LULC classes. We calculated transition probabilities for two different time phases. The first phase is from 2008 to 2015, with an eight-year interval, whereas the second phase denotes 27-year interval from 1994 to 2020 (Table 3). The comparison between the two-time phases reveals a similar trend in the transition probabilities for different LULC feature classes. However, remarkable transformations were reported in the second phase for the majority of the classes. The analysis of the transition probability matrix for 2008–2015 shows that forest and agricultural lands have more prospects to change into built-up lands with probabilities of 0.207 and 0.3 than other land use types. The likelihood of modifying fallow lands into water bodies and forests are 0.1 and 0.12, respectively. Forest cover indicates a probability of 0.14 for its alteration into agricultural lands in the same period (Table 3). The LULC transition between two same classes (e.g. water body to water body, urban lands to urban lands) refers to the probability of no change in the class for the time interval. For instance, the likelihood of urban land remaining the same is 0.77 from 2008 to 2015, which indicates that 77% of the pixel remains unchanged for that particular class in that particular duration (Table 3). Likewise, the transition probability between two classes during a specific time interval indicates the chances of shifting from one class to another. For example, we found the transition probability of 0.3 between agricultural land and built-up land between 2008 and 2015, which denotes that 30% pixels from the agricultural land cover type of 2008 are prone to convert into built-up lands by the year 2015. During the period 1994–2020, the fallow lands were

Table 3 Transition probability statistics of LULC features from 2008 to 2015 and 1994 to 2020

LULC type	Water bodies		Fallow lands		Forest		Agricultural lands		Built-up lands	
	2008–2015	1994–2020	2008–2015	1994–2020	2008–2015	1994–2020	2008–2015	1994–2020	2008–2015	1994–2020
Water bodies	0.95	0.8749	0.05	0.09	0.0007	0.0122	0.0017	0.0066	0.0015	0.016
Fallow lands	0.1	0.068	0.66	0.34	0.12	0.2	0.06	0.236	0.06	0.142
Forest	0.0004	0.00144	0.018	0.026	0.635	0.5	0.14	0.116	0.207	0.36
Agricultural lands	0.0054	0.0017	0.012	0.024	0.162	0.244	0.524	0.28	0.3	0.45
Built-up lands	0.001	0.002	0.017	0.033	0.09	0.14	0.13	0.23	0.77	0.6

modified into forest, agricultural lands, and built-up lands, with probabilities of 0.2, 0.236, and 0.142. The chances of forest cover converting to agricultural lands and built-up lands were found to be 0.116 and 0.36. The agricultural lands are highly susceptible to transformation into built-up lands, as indicated with a high transition probability value of 0.45. On average, the probability of getting converted into built-up lands from other classes is remarkable, reducing the pervious cover in the study area.

Model validation

During the analysis, three different maps, viz., transition potential map, certainty raster, and simulated LULC map were generated. These maps were produced with the outputs from the CA after the transition potential modelling using the memory from the MLP-ANN algorithm. The changes associated with corresponding LULC (e.g. forest to built-up land transition potential, forest to agricultural land transition potential, forest to barren transition potential, and forest to water body transition probability) were used to construct a transition potential map. The certainty raster refers to the change between two large transition potentials, which depends on the LULC classes and the transition potential. Transition potential denotes the certainty of occurrence in the predicted LULC map. The greater the change in the certainty raster, the higher is the confidence in the simulated map. Before simulation of future patterns in the LULC using the CA–Markov model, the model has been validated with a simulated 2020 LULC map as shown in Fig. 7b.

Comparison of the areal statistics for the LULC features between observed and simulated data of the year 2020 was performed for each class individually and represented in Fig. 7c. The comparison also states that the model over predicts the values in agricultural land type and built-up lands, whereas under predicted values are obtained from the model for the forest, water bodies, and fallow lands.

The results were validated by comparing the simulated and the observed LULC map of 2020 (Fig. 7). Kappa statistics were computed from these observed and simulated maps of 2020. The statistics showed K_{loc} as 0.77, $K_{overall}$ as 0.72, K_{histo} as 0.94, and the overall percentage of correctness was observed to be 87.5%. The coupled MLP-CA–Markov model results presented good simulation outputs, with kappa coefficient values and overall accuracy higher than 0.7, hence the model to be reliable for the present study region.

Projection of future LULC scenarios

After validation, we adopted the model to predict the LULC scenarios of 2045, 2073, and 2100. The spatial distribution of simulated LULC future scenarios is represented in Fig. 8. The areal statistics of future projection

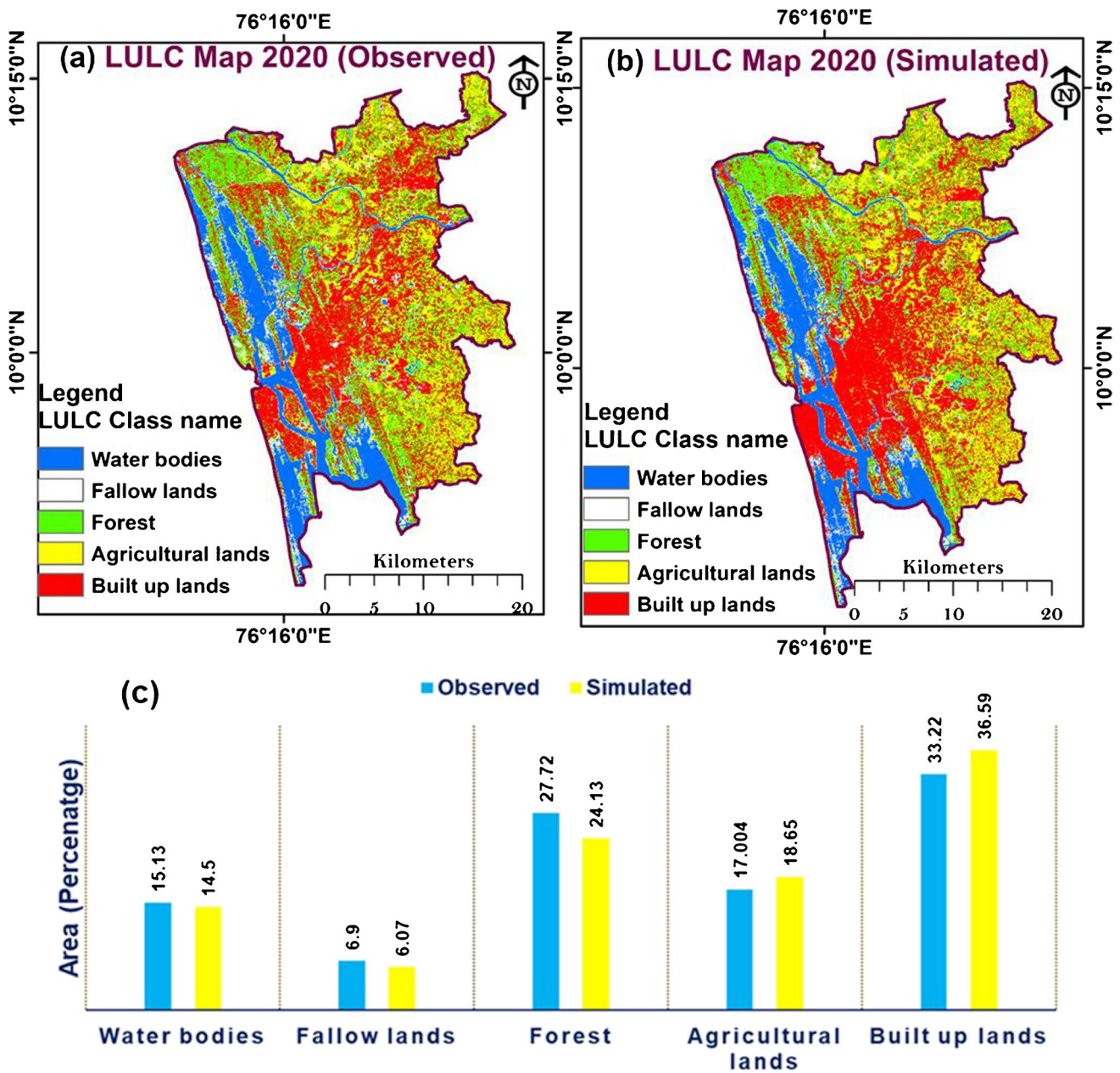


Fig. 7 LULC map of 2020. (a) derived from satellite data, (b) simulated using CA–Markov model, and (c) comparison of areal statistics of LULC features from satellite-derived and simulated maps for the year 2020

are illustrated in Fig. 9 and Table 4. The result predicted a significant increase in the areal extent of built-up land during 2020–2100, along with a considerable loss in natural land cover such as forest and agricultural lands (Table 4). The model predicted a slight reduction in fallow land (6.9 to 4.53%) and water bodies (15.13 to 14.96%). The complete analysis of the predicted results indicates a need for more significant fortification of the environment and preservation of natural land cover and associated rare, vulnerable species in the study area. Moreover, the region is among the twelve districts of Kerala, which falls under

the Western Ghats expanse and is one of the World’s eight biodiversity spots.

The FLULC for different periods 2045, 2073, and 2100 (Fig. 8) were generated following the successful simulation of LULC changes in 2020 (Fig. 7b). The annual change rate in each LULC type was computed with Eq. (5). Figure 10 denotes the future LULC statistics and the rate of change (gain/loss) in each class at an annual scale for different time phases (Table 4).

The maximum annual growth rate of 1.95% was predicted for built-up lands between 2020 and 2045, 0.4% was

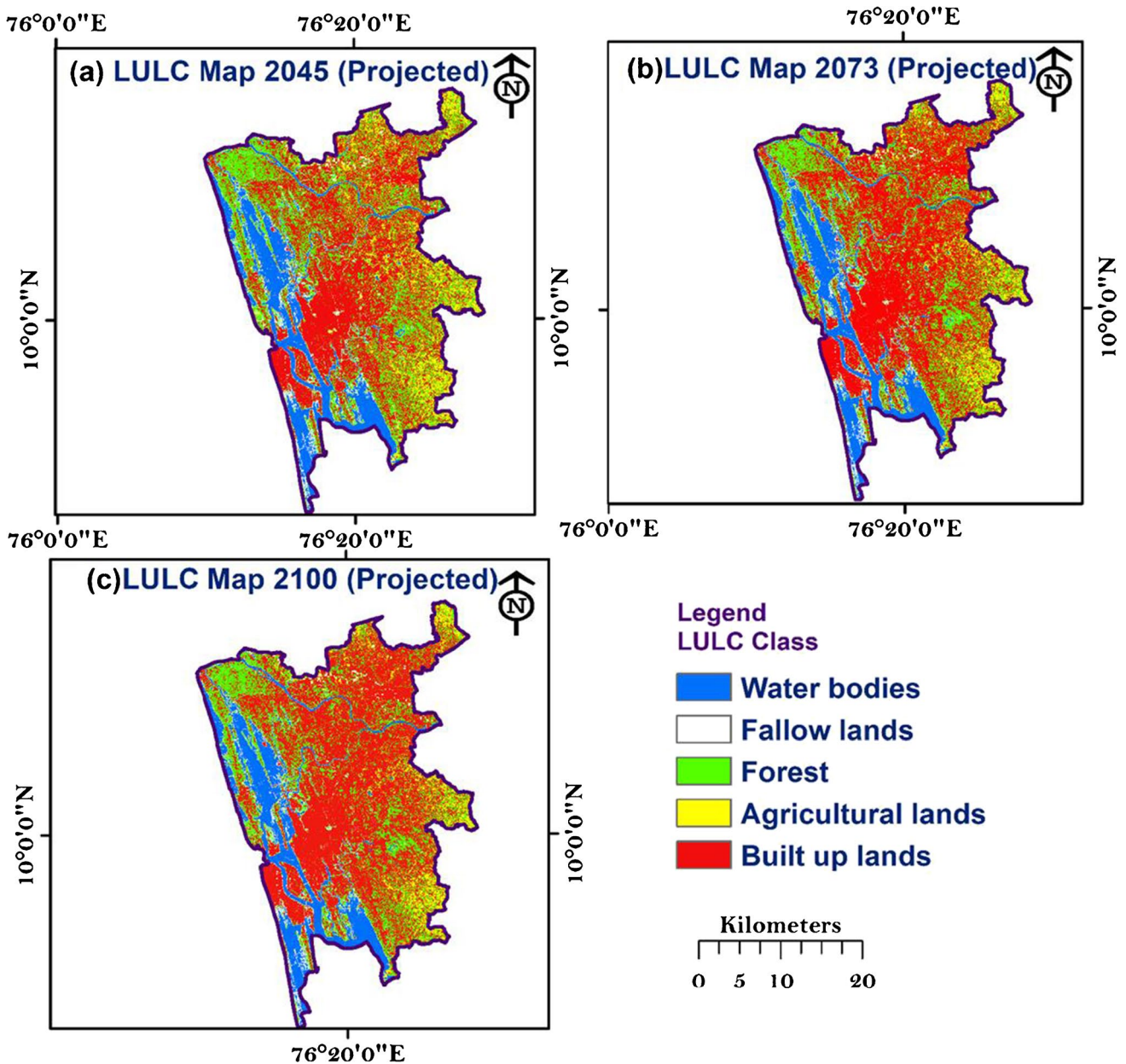


Fig. 8 Projected LULC maps for future (a) 2045, (b) 2073, and (c) 2100

predicted between 2045 and 2073, and 0.23% between 2073 and 2100. The maximum urbanisation was expected to happen during 2020–2045, i.e. in the near future. The model also predicted the overall annual growth rate in built-up land to be 0.79% per year from 1994 to 2100 (Fig. 10 and Table 4).

The maximum annual decreasing rate was predicted in agricultural land with an average rate of 1.75% per year between 2020 and 2045 (near future), 1.13% in the middle future (2045–2073), and 1.6% in the far future (2073–2100), indicating the significant declination in the near and far future. The model predicts a decreasing trend for the forest

cover scenario with an annual rate of 1.12% per year, 0.46% per year, and 0.16% per year in the near, middle, and far future, respectively. The fallow lands are predicted to show an annual trend of 0.56% per annum decrease between 2020 and 2045, whereas the other phases have a very slight decreasing rate of 0.01% per year (Table 4). The water bodies are predicted to have a decreasing trend of shallow magnitude (Fig. 10 and Table 4).

Furthermore, we analysed the surface area proportions of pervious with respect to impervious from the derived LULC maps. It is observed that there is a constantly rising trend in the pervious to impervious surface proportions during the

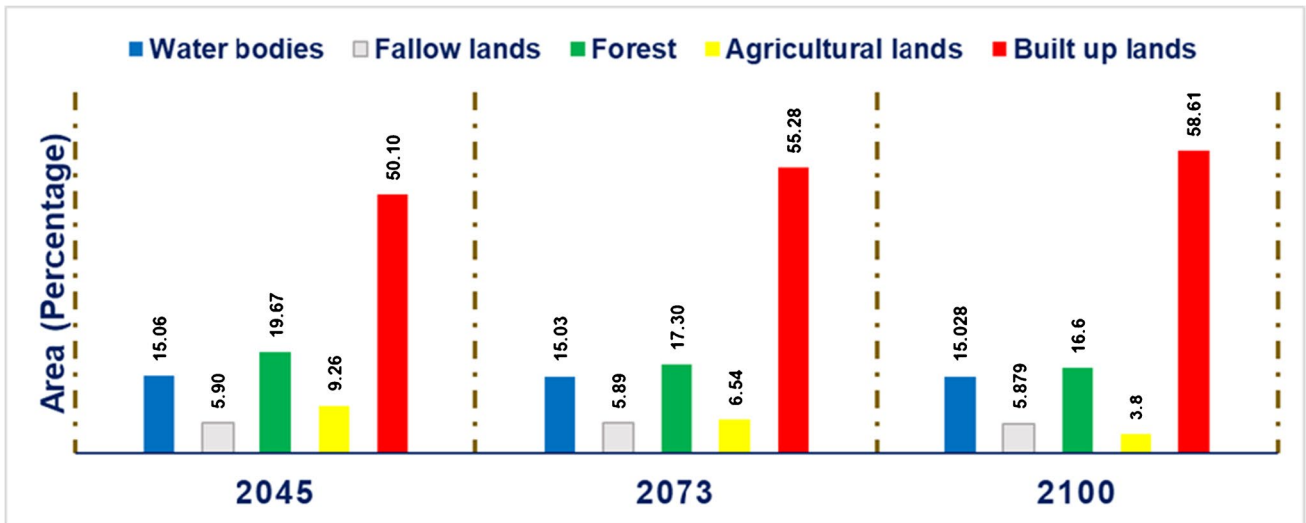


Fig. 9 Change detection for the LULC features between 2045 and 2100

Table 4 Annual change rate (%) estimation in LULC for various phases from 2020 to 2100

LULC classes	Total projected area cover (km ²)				DD (%) between different time periods			
	2020	2045	2073	2100	2020–2045	2045–2073	2073–2100	2020–2100
Water bodies	136.37	134.19	132.81	132.75	-0.02	-0.01	0.00	-0.03
Fallow lands	62.27	48.12	41.8	40.96	-0.56	-0.01	-0.01	-0.44
Forest	249.8	252.44	236.03	201.6	-1.12	-0.46	-0.16	-0.25
Agricultural lands	153.22	76.29	51.35	45.67	-1.75	-1.13	-1.61	-0.90
Built-up lands	299.43	392.95	442	483	1.95	0.40	0.23	0.79

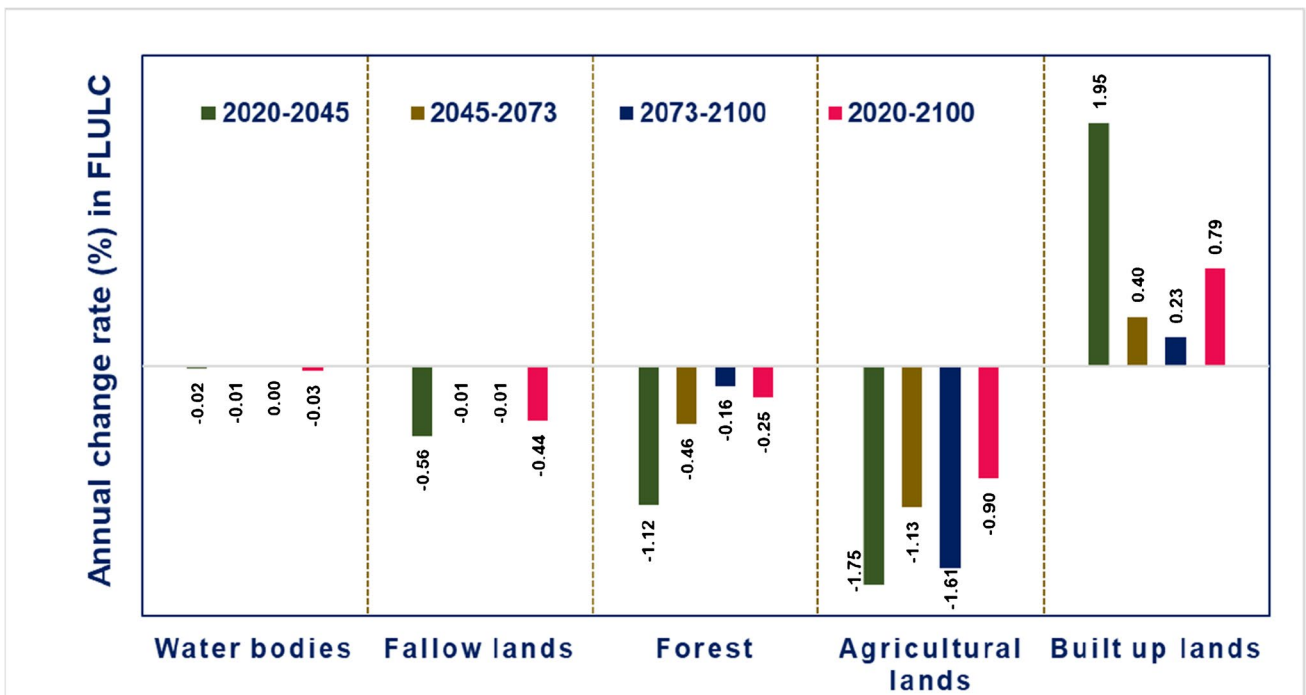


Fig. 10 Annual change rate (%) of each Future Land Use Land Cover type at various phases

study period for the last three decades (1994–2020). Additionally, we found that this trend is increasing at an alarming rate for the projected future scenarios. In 1994, the proportion of pervious land was about 90%, and around 9% was impervious. For the recent 2020 scenario, the proportion of impervious areas increased to around 30%. However, the predicted results for 2100 rose to 58% for the impervious surface area with a reduction of 41% for the pervious surface area (Fig. 11). The computed ratio of impervious surface area to the pervious showed a drastic increase from 0.1 in 1994 to 0.5 in 2020 to 1.42 in 2100.

From the analysis, the major alterations in LULC are predicted during the near future phase (2020–2045), which indicates a higher rate of decrease in the pervious surface. The rapid growth of urbanisation and other anthropogenic activities have affected all major LULC classes such as water bodies, forest, fallow lands, and agricultural lands from 2020 to 2100. The LULC map of the year 2100 indicates a vast decrease in the pervious surface area, pointing to a potentially dangerous environment in the future across the study area. The destruction of the natural land cover indicates the need for long-term landscape maintenance and development.

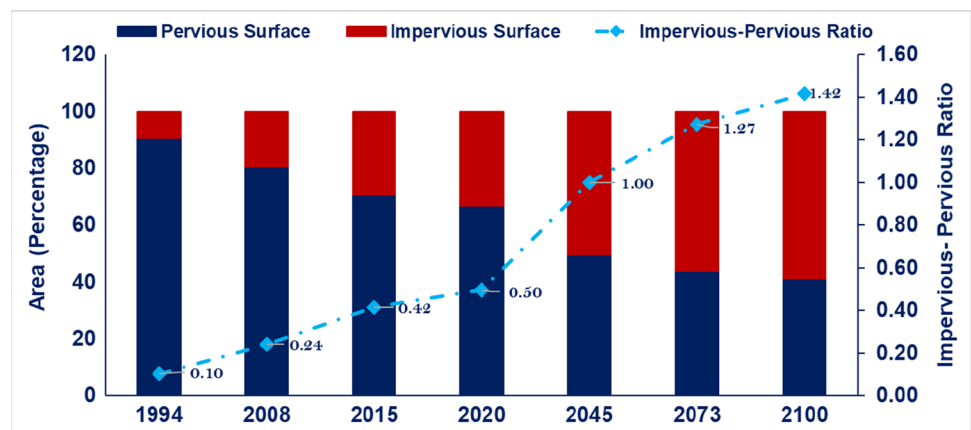
Significant growth in the built-up area has been observed in the Cochin and Kanayannur talukas of the study area. Many major and minor industrial development projects have been initiated and established in Cochin in the past fifteen years (George 2016). Financial development and urban population growth resulted in rapid urbanisation of the study area. The high rate of migration from other parts of India leads to the development and expansion of slums on the periphery of development centres, which is an unavoidable result of unplanned city development. The increased urban population exerts pressure on natural land cover in order to meet infrastructure requirements. Previous research suggests that LULC changes in peri-urban areas take the form of built-up expansion at the cost of agricultural land, forest, vegetation cover, and

fallow lands (Kale et al. 2016; Naikoo et al. 2020; Obeidat et al. 2019; Patra et al. 2018). Following the commencement of Jawaharlal Nehru National Urban Renewal Mission (JNNURM) of the Government of India, Cochin and its surrounding peri-urban areas have witnessed massive changes in LULC (Aravindan and Prasanth 2018; George 2016).

Moreover, the natural land cover such as agricultural lands, forests, fallow, and water bodies has significantly reduced its area. Agricultural and forest land are the main land use types that have experienced the most adverse change and are being converted into built-up land as part of the urban infrastructure development process (Devi and Nair 2021; Dipson et al. 2015; Krishnan and Firoz 2021; Nair et al. 2016). In a recent study conducted by Dipson et al. (2015), it was mentioned that the estuaries (Cochin backwater) in the study area had been reduced due to the development activities and real estate boom. Similarly, Shaji et al. (2017) observed a significant decline in agricultural, mangrove, and barren lands due to increased built-up lands in Cochin.

Among all natural resources, the land is the most important and readily accessible resource for humans and is used in numerous ways and for various applications. Hence, population change directly impacts the LULC pattern of a region (Naikoo et al. 2020; Showqi et al. 2014; Wang et al. 2021a, b, c). The majority of population changes happen as a result of natural population growth or migration. Massive migration to urban areas is the main driver for urban population growth in the current study area, and it is expected to extend further. The main national and international commercial activities, such as chemical industries, harbour exports, imports, information technology (IT), and tourism, attract many labours towards the study area. Hence, in recent three decades, an urban population rise and the expansion of the tertiary sector are considerably changing the LULC pattern of Cochin.

Fig. 11 Variations in the pervious and impervious surface areas between 1994 and 2100



Model limitations

There are possible limitations with the model study despite effective simulations and consistent outputs. The accuracy of the simulated results is affected by several factors which incorporate several uncertainties in the predicted results. Firstly, there are chances of systematic biases in the input raster due to the different sensor systems involved in the satellite image acquisition (Lu et al. 2019). The classification accuracy of LULC maps used in this study is different, due to which independent mistakes might disturb the forecast precision of the model. The simulated results have a higher convergence to the Landsat data, but the consistency in prediction accuracy varies with the satellite data, thereby incorporating model uncertainties. The comparison also states that the model over predicts the values in the case of agricultural land type and built-up lands, whereas it underpredicts the values for the forest, water bodies, and fallow-lands.

Additionally, the drivers chosen for the simulations were thorough but not exhaustive. Several factors such as the economy, global legislation, and administrative resolutions were not considered. The use of an increased number of drivers can enhance the model's ability to forecast the changes across the area (Kale et al. 2016).

Conclusions

This study attempts to forecast future LULC scenarios for a highly urbanised Cochin region in Ernakulam district using the MOLUSCE module in the QGIS platform. The LULC dynamics are analysed and modelled successfully with the integration of GIS techniques and MOLUSCE. Furthermore, MOLUSCE was integrated with the MLP-ANN algorithm and cellular-automata-Markov model to attain better simulation results. We used the maximum likelihood classification technique for the LULC map generation from 1994 to 2020 with Landsat data. The spatiotemporal analysis of LULC maps indicates substantial growth in the built-up land with decreasing natural land cover for the mentioned period. The socio-economic development and human encroachments in the natural land cover have intensified the changes in the LULC.

Additionally, computation of the annual growth rate in terms of the dynamic degree of LULC yields an overall decreasing trend in the natural land cover such as forest, agricultural land, fallow lands, and water bodies at annual rates of -0.71% per year, -1.68% per year, -1.19% per year, and -0.26% per year, respectively. Moreover, the development of built-up land is primarily around the estuaries of the region. Estuaries are the most ecologically sensitive zones in the chosen study area. We derived the LULC transition

potential using the classified LULC maps along with the driving factors such as DEM, slope, distance from roads, distance from water bodies, and population density in the MLP-ANN algorithm. The future LULC maps were forecasted with the simulation of the CA-Markov model. The model performance was tested by comparing the observed with the simulated LULC map of 2020 using kappa statistics and overall accuracy. The model reliability is known from the overall accuracy of 87.5%, with the kappa statistics higher than 0.7.

Following the validation, the MLP-ANN algorithm is used to simulate future transformations in 2045, 2073, and 2100. CA Markov model was used to predict future LULC maps for the corresponding years. The results predict a drastic increase in urbanisation for the study area in the immediate next 25 years with high rate of deforestation and degradation of agricultural fields. From 1994 to 2100, a substantial shift of pervious surface to the impervious surface was observed (0.1 to 1.42). Therefore, the development and implementation of a reasonable land use policy can reduce the threat of degradation of natural resources, and it will be helpful in sustainable development. The governments may be advised to pay immediate attention to rigorous land expansion, and maintain regulations in land use for development activities, as they are often the primary triggers to the environmental balance disturbance. This study can offer strategic guidance to urban and rural land use planners to achieve efficient land use management.

Supplementary Information The online version contains supplementary material available at <https://doi.org/10.1007/s12517-022-09735-7>.

Acknowledgements The authors would like to express their sincere thanks to the Indian Institute of Technology Guwahati, India, and the National Centre for Earth Science Studies (NCESS), Thiruvananthapuram, India, for providing facilities for the study.

Funding The research work was funded by the National Centre of Earth Science Studies under the Ministry of Earth Sciences, Govt. of India (Grant No NCESS project D/GW).

Availability of data The data used to support the findings of this study are included in the article.

Declarations

Conflict of interest The authors declare no competing interests.

References

- Al A, Rahman S, Faisal A (2020) Modelling future land use land cover changes and their impacts on land surface temperatures in Rajshahi, Bangladesh. *Remote Sens Appl Soc Environ* 100314. <https://doi.org/10.1016/j.rsase.2020.100314>

- Amini Parsa V, Salehi E (2016) Spatio-temporal analysis and simulation pattern of land use/cover changes, case study: Naghadeh. Iran J Urban Manag 5(2):43–51. <https://doi.org/10.1016/j.jum.2016.11.001>
- Aneesha Satya B, Shashi M, Deva P (2020) Future land use land cover scenario simulation using open source GIS for the city of Warangal, Telangana. India Appl Geomatics 12(3):281–290. <https://doi.org/10.1007/s12518-020-00298-4>
- Aravindan A, Prasanth WCB (2018) Changing paradigm of Kerala's urbanisation model with special reference to JNNURM at Ernakulam District. Int J Manag Stud V(Special Issue 1): <https://doi.org/10.18843/ijms/v5is1/02>
- Chanapathi T, Thatikonda S (2020) Investigating the impact of climate and land-use land cover changes on hydrological predictions over the Krishna river basin under present and future scenarios. Sci Total Environ 721:137736. <https://doi.org/10.1016/j.scitotenv.2020.137736>
- Congalton RG (1991) A review of assessing the accuracy of classifications of remotely sensed data. Remote Sens Environ 37(1):35–46. [https://doi.org/10.1016/0034-4257\(91\)90048-B](https://doi.org/10.1016/0034-4257(91)90048-B)
- Datta P (2006) Urbanisation in India. European Population Conference; chrome-extension://efaidnbmnnnibpcajpcgclefndmkaj/viewer.html?pdfurl=http%3A%2F%2Flibrary.isical.ac.in%3A8080%2Fjspuif%2Fbitstream%2F10263%2F2460%2F1%2Furbanisation%2520in%2520india.pdf&clen=197962
- Department of Mining and Geology (2016) District survey report of minor minerals, Ernakulam, Thiruvananthapuram, Government of Kerala: http://www.dmg.kerala.gov.in/docs/pdf/dsr/dsr_ern.pdf
- Devi AB, Nair AM (2021) Effects of urbanization in a shallow coastal aquifer: an integrated GIS-based case study in Cochin, India. Groundw Sustain Dev: 100656. <https://doi.org/10.1016/j.gsd.2021.100656>
- Dipson PT, Chithra SV, Amarnath A, Smitha SV, Harindranathan Nair MV, Shahin A (2015) Spatial changes of estuary in Ernakulam district, Southern India for last seven decades, using multi-temporal satellite data. J Environ Manage 148:134–142. <https://doi.org/10.1016/j.jenvman.2014.02.021>
- Fichera CR, Modica G, Pollino M (2017) Land Cover classification and change-detection analysis using multi-temporal remote sensed imagery and landscape metrics. Eur J Remote Sens 7254. <https://doi.org/10.5721/EuJRS20124501>
- Fondevilla C, Àngels Colomer M, Fillat F, Tappeiner U (2016) Using a new PDP modelling approach for land-use and land-cover change predictions: a case study in the Stubai Valley (Central Alps). Ecol Modell 322:101–114. <https://doi.org/10.1016/j.ecolmodel.2015.11.016>
- Foody GM (2002) Status of land cover classification accuracy assessment. Remote Sens Environ 80(1):185–201. [https://doi.org/10.1016/S0034-4257\(01\)00295-4](https://doi.org/10.1016/S0034-4257(01)00295-4)
- Fox TA, Rhemtulla JM, Ramankutty N, Lesk C, Coyle T, Kunhamu TK (2017) Agricultural land-use change in Kerala, India: perspectives from above and below the canopy. Agric Ecosyst Environ 245(May):1–10. <https://doi.org/10.1016/j.agee.2017.05.002>
- Gao J, O'Neill BC (2020) Mapping global urban land for the 21st century with data-driven simulations and Shared Socioeconomic Pathways. Nat Commun 11(1):1–12. <https://doi.org/10.1038/s41467-020-15788-7>
- George J (2016) An assessment of inclusiveness in the urban agglomeration of Kochi City: the need for a change in approach of urban planning
- Gharaibeh A, Shaamala A, Obeidat R, Al Kofahi S (2020) Improving land-use change modelling by integrating ANN with Cellular Automata-Markov Chain model. Heliyon 6(9):e05092. <https://doi.org/10.1016/j.heliyon.2020.e05092>
- Guidigan MLG, Sanou CL, Ragatoa DS, Fafa CO, Mishra VN (2019) Assessing land use/land cover dynamic and its impact in Benin Republic using land change model and CCI-LC products. Earth Syst Environ 3(1):127–137. <https://doi.org/10.1007/s41748-018-0083-5>
- Hakim AMY, Baja S, Rampisela DA, Arif S (2019) Spatial dynamic prediction of landuse / landcover change (case study: Tamalanrea sub-district, makassar city). IOP Conf Ser Earth Environ Sci 280(1): <https://doi.org/10.1088/1755-1315/280/1/012023>
- Ibrahim WYW, Ludin ANM (2015) Spatiotemporal land use change analysis using open-source GIS and web based application. Int J Sustain Built Environ 2(2):101–107
- Jogun T, Lukić A, Gašparović M (2019) Simulation model of land cover changes in a post-socialist peripheral rural area: Požež-slavonia county, Croatia. Hrvat Geogr Glas 81(1): 31–59. <https://doi.org/10.21861/HGG.2019.81.01.02>
- John J, Bindu G, Srimuruganandam B, Wadhwa A, Rajan P (2020) Land use/land cover and land surface temperature analysis in Wayanad district, India, using satellite imagery. Ann GIS 26(4):343–360. <https://doi.org/10.1080/19475683.2020.1733662>
- Johnson D (2018) Cropping pattern changes in Kerala, 1956–57 to 2016–17. Rev Agrar Stud 8(1)
- Kafy AA, Dey NN, Al Rakib A, Rahaman ZA, Nasher NMR, Bhatt A (2021) Modelling the relationship between land use/land cover and land surface temperature in Dhaka. Bangladesh using CA-ANN algorithm. Environ Challenges 4(May):100190. <https://doi.org/10.1016/j.envc.2021.100190>
- Kale MP, Chavan M, Pardeshi S, Joshi C, Verma PA, Roy PS, Srivastav SK, Srivastava VK, Jha AK, Chaudhari S, Giri Y, Krishna Murthy YVN (2016) Land-use and land-cover change in Western Ghats of India. Environ Monit Assess 188(7): <https://doi.org/10.1007/s10661-016-5369-1>
- Krishnan VS, Firoz CM (2021) Impact of land use and land cover change on the environmental quality of a region: a case of Ernakulam district in Kerala, India. Reg Stat 11(2): 102–135. <https://doi.org/10.15196/RS110205>
- Leta MK, Demissie TA, Tränckner J (2021) Modelling and prediction of land use land cover change dynamics based on land change modeler (Lcm) in nashe watershed, upper blue Nile basin, Ethiopia. Sustain 13(7): <https://doi.org/10.3390/su13073740>
- Li B, Shi X, Lian L, Chen Y, Chen Z, Sun X (2020) Quantifying the effects of climate variability, direct and indirect land use change, and human activities on runoff. J Hydrol 584(February):124684. <https://doi.org/10.1016/j.jhydrol.2020.124684>
- Lu Y, Wu P, Ma X, Li X (2019) Detection and prediction of land use/land cover change using spatiotemporal data fusion and the Cellular Automata-Markov model. Environ Monit Assess 191(2): <https://doi.org/10.1007/s10661-019-7200-2>
- Mohan M, Pathan SK, Narendrareddy K, Kandy A, Pandey S (2011) Dynamics of urbanisation and its impact on land-use/land-cover: a case study of megacity Delhi. J Environ Prot 02(09):1274–1283. <https://doi.org/10.4236/jep.2011.29147>
- Mozumder C, Tripathi NK, Losiri C (2016) Comparing three transition potential models: a case study of built-up transitions in North-East India. Comput Environ Urban Syst 59:38–49. <https://doi.org/10.1016/j.compenvurbsys.2016.04.009>
- Naikoo MW, Rihan M, Ishtiaque M, Shahfahad, (2020) Analyses of land use land cover (LULC) change and built-up expansion in the suburb of a metropolitan city: spatio-temporal analysis of Delhi NCR using landsat datasets. J Urban Manag 9(3):347–359. <https://doi.org/10.1016/j.jum.2020.05.004>
- Nair AM, Mohanlal L, Nabeela CA, Aneesh TD, Srinivas R (2016) Study on the impact of land use changes on urban hydrology of Cochin, Kerala, India. In Urban Hydrology, Watershed Management and Socio-Economic Aspects (pp. 69–82). Springer, Cham

- Nath B, Ni-Meister W, Choudhury R (2021) Impact of urbanisation on land use and land cover change in Guwahati city, India and its implication on declining groundwater level. *Groundw Sustain Dev* 12(October 2020):100500. <https://doi.org/10.1016/j.gsd.2020.100500>
- Nath B, Wang Z, Ge Y, Islam K, Singh RP, Niu Z (2020) Land use and land cover change modelling and future potential landscape risk assessment using Markov-CA model and analytical hierarchy process. *ISPRS Int J Geo-Information* 9(2): <https://doi.org/10.3390/ijgi9020134>
- Obeidat M, Awawdeh M, Lababneh A (2019) Assessment of land use/land cover change and its environmental impacts using remote sensing and GIS techniques, Yarmouk River Basin, north Jordan. *Arab J Geosci* 12(22): <https://doi.org/10.1007/s12517-019-4905-z>
- Patra S, Sahoo S, Mishra P, Mahapatra SC (2018) Impacts of urbanisation on land use /cover changes and its probable implications on local climate and groundwater level. *J Urban Manag* 7(2):70–84. <https://doi.org/10.1016/j.jum.2018.04.006>
- Pijanowski BC, Brown DG, Shellito BA, Manik GA (2002) Using neural networks and GIS to forecast land use changes: a land transformation model. *Comput Environ Urban Syst* 26(6):553–575
- Rafeeqe MK, Rameshan M, Sreeraj MK (2020) Measuring the vulnerability of coastal ecosystems in a densely populated west coast landscape, India: a remote sensing perspective. In *Remote Sensing of Ocean and Coastal Environments* (pp. 203–224). Elsevier
- Rahman MTU, Tabassum F, Rasheduzzaman M, Saba H, Sarkar L, Ferdousn J, Uddin, SZ, Zahedul Islam AZM (2017) Temporal dynamics of land use/land cover change and its prediction using CA-ANN model for southwestern coastal Bangladesh. *Environ Monit Assess* 189(11): <https://doi.org/10.1007/s10661-017-6272-0>
- Reddy CS, Singh S, Dadhwal VK, Jha CS, Rao NR, Diwakar PG (2017) Predictive modelling of the spatial pattern of past and future forest cover changes in India. *J Earth Syst Sci* 126(1): <https://doi.org/10.1007/s12040-016-0786-7>
- Rodrigues E, Guimar CA (2021) Land Use Policy Future scenarios based on a CA-Markov land use and land cover simulation model for a tropical humid basin in the Cerrado / Atlantic forest ecotone of Brazil. *Land use policy* 101(February 2020): <https://doi.org/10.1016/j.landusepol.2020.105141>
- Sajeev R, Subramanian V (2003) Land use/land cover changes in Ashtamudi wetland region of Kerala - a study using remote sensing and GIS. *J Geol Soc India* 61(5):573–580
- Samal DR, Gedam SS (2013) Monitoring land use changes associated with urbanisation in the upper Bhima basin, Maharashtra, India. *International Geoscience and Remote Sensing Symposium (IGARSS)* 2673–2676. <https://doi.org/10.1109/IGARSS.2013.6723373>
- Sang L, Zhang C, Yang J, Zhu D, Yun W (2011) Simulation of land use spatial pattern of towns and villages based on CA-Markov model. *Math Comput Model* 54(3–4):938–943. <https://doi.org/10.1016/j.mcm.2010.11.019>
- Sankarrao L, Ghose DK, Rathinsamy M (2021) Predicting land-use change: intercomparison of different hybrid machine learning models. *Environ Model Softw* 145(September):105207. <https://doi.org/10.1016/j.envsoft.2021.105207>
- Shaji Jithu, SL Sajith, Jyoti Joseph, KK Ramachandran (2017) LULC change along Central Kerala coast and perception on implementation of CRZ Notification. *National Conference on Geospatial Technology*. <https://www.researchgate.net/publication/312471897>
- Showqi I, Rashid I, Romshoo SA (2014) Land use land cover dynamics as a function of changing demography and hydrology. *GeoJournal* 79(3):297–307. <https://doi.org/10.1007/s10708-013-9494-x>
- Singh SK, Mustak S, Srivastava PK, Szabó S, Islam T (2015) Predicting spatial and decadal LULC changes through cellular automata Markov chain models using earth observation datasets and geo-information. *Environ Process* 2(1):61–78. <https://doi.org/10.1007/s40710-015-0062-x>
- Sisodia PS, Tiwari V, Kumar A (2014) Analysis of supervised maximum likelihood classification for remote sensing image. *Int Conf Recent Adv Innov Eng* 2014:9–12. <https://doi.org/10.1109/ICRAIE.2014.6909319>
- Sohl TL, Wimberly MC, Radeloff VC, Theobald DM, Sleeter BM (2016) Divergent projections of future land use in the United States arising from different models and scenarios. *Ecol Modell* 337:281–297. <https://doi.org/10.1016/j.ecolmodel.2016.07.016>
- Sreelekshmi S, Veettil BK, Bijoy Nandan S, Hari Krishnan M (2021) Mangrove forests along the coastline of Kerala, southern India: current status and future prospects. *Reg Stud Mar Sci* 41:101573. <https://doi.org/10.1016/j.rsma.2020.101573>
- State urbanisation report (2012) A study on the scattered human settlement pattern of Kerala and its development issues Thiruvananthapuram, Government of Kerala: <https://townplanning.kerala.gov.in/town/wp-content/uploads/2018/12/SUR.pdf>
- Sun J, Yang J, Zhang C, Yun W, Qu J (2013) Automatic remotely sensed image classification in a grid environment based on the maximum likelihood method. *Math Comput Model* 58(3–4):573–581. <https://doi.org/10.1016/j.mcm.2011.10.063>
- Tahiru AA, Doke DA, Baatuwuwie BN (2020) Effect of land use and land cover changes on water quality in the Nawuni Catchment of the White Volta Basin, Northern Region. *Ghana Appl Water Sci* 10(8):1–14. <https://doi.org/10.1007/s13201-020-01272-6>
- Thomas JS 2017 A study on urbanisation of Kerala with reference to the cities and the slum population. *technology*, 49(Part 4)
- Unwin A, Isaacson DL, Madsen RW (1977) Markov chains -- theory and applications. *Oper Res Q* (1970–1977) 28(1): 236. <https://doi.org/10.2307/3008804>
- Vadrevu KP, Justice C, Prasad N, Gutman G (2015) Land cover/land use change and impacts on environment in South Asia. *J Environ Manage* 148(November 2017):1–3. <https://doi.org/10.1016/j.jenvman.2014.12.005>
- Wang K, Tong Y, Gao J, Gao C, Wu K, Yue T, Qin S, Wang C (2021a) Impacts of LULC, FDDA, Topo-wind and UCM schemes on WRF-CMAQ over the Beijing-Tianjin-Hebei region. *China Atmos Pollut Res* 12(2):292–304. <https://doi.org/10.1016/j.apr.2020.11.011>
- Wang Q, Guan Q, Lin J, Luo H, Tan Z, Ma Y (2021b) Simulating land use/land cover change in an arid region with the coupling models. *Ecol Indic* 122:107231. <https://doi.org/10.1016/j.ecoli.2020.107231>
- Wang W, Chen Y, Wang W, Jiang J, Cai M, Xu Y (2021c) Evolution characteristics of groundwater and its response to climate and land-cover changes in the oasis of dried-up river in Tarim Basin. *J Hydrol* 594(818):125644. <https://doi.org/10.1016/j.jhydrol.2020.125644>
- Waseem M, Halmy A, Gessler PE, Hicke JA, Salem BB (2015) Land use / land cover change detection and prediction in the north-western coastal desert of Egypt using Markov-CA. *Appl Geogr* 63:101–112. <https://doi.org/10.1016/j.apgeog.2015.06.015>
- Yang X, Chen R, Zheng XQ (2016) Simulating land use change by integrating ANN-CA model and landscape pattern indices. *Geomatics Nat Hazards Risk* 7(3):918–932. <https://doi.org/10.1080/19475705.2014.1001797>

- Yonaba R, Koïta M, Mounirou LA, Tazen F, Queloz P, Biao AC, Niang D, Zouré C, Karambiri H, Yacouba H (2021) Spatial and transient modelling of land use/land cover (LULC) dynamics in a Sahelian landscape under semi-arid climate in northern Burkina Faso. *Land Use Policy*, 103(August 2020): <https://doi.org/10.1016/j.landusepol.2021.105305>
- Yuan F (2008) Land-cover change and environmental impact analysis in the Greater Mankato area of Minnesota using remote sensing and GIS modelling. *Int J Remote Sens* 29(4):1169–1184. <https://doi.org/10.1080/01431160701294703>
- Zhang YK, Schilling KE (2006) Effects of land cover on water table, soil moisture, evapotranspiration, and groundwater recharge: a field observation and analysis. *J Hydrol* 319(1–4):328–338. <https://doi.org/10.1016/j.jhydrol.2005.06.044>